2008-01-07

Air-Trench Splitters for Ultra-Compact Ring Resonators in Low Refractive Index Contrast Waveguides

Seunghyun Kim

Gregory P. Nordin
nordin@byu.edu

Yongbin Lin

Nazli Rahmanian

Original Publication Citation

N. Rahmanian, S. Kim, Y. Lin, G. P. Nordin, "Air-trench splitters for ultra-compact ring resonators in low refractive index contrast waveguides," Optics Express 16(1), pp. 456-465 (28). http://www.opticsexpress.org/abstract.cfm?id=14878.

Air-trench splitters for ultra-compact ring resonators in low refractive index contrast waveguides

Nazli Rahmanian,[1] Seunghyun Kim,[2] Yongbin Lin, [1] and Gregory P. Nordin[2]

[1]*Nano and Micro Devices Center, University of Alabama in Huntsville, Huntsville AL 35899 USA*
[2]*Electrical and Computer Engineering, Brigham Young University, Provo, UT 84602 USA*
nordin@ee.byu.edu

Abstract: We demonstrate air-trench splitters in low index contrast perfluorocyclobutyl (PFCB) waveguides. Splitters are fabricated by etching 800 nm wide high aspect ratio (18:1) trenches. The measured optical loss is 0.4 dB/splitter. The reflection/transmission splitting ratio is 0.859/0.141, which closely matches two-dimensional finite difference time domain (2D-FDTD) simulation results. Air-trench splitters and bends are used to demonstrate an ultra-compact ring resonator (RR) with a size reduction of 1,700 compared to a RR based on traditional curved waveguides in the same material system. A comparison between the RR's measured and analytically calculated performance shows close agreement when splitter and bend losses are taken into account.

OCIS codes: (130.0130) Integrated optics; (130.5460) Polymer waveguides; (230.1360) Beam splitters; (230.5750) Resonators; (250.5300) Photonic integrated circuits

References and links

1. D. -G. Sun, Y. Zha, T. Liu, Y. Zhang, X. Li, and X. Fu, "Demonstration for rearrangeable nonblocking 8×8 matrix optical switches based on extended banyan networks," Opt. Express **15,** 9347-9356 (2007).
2. W. Lin, C. J. Sun, and K. M. Schmidt, "Hybrid integration platform based on silica on silicon planar lightwave circuits," Proc. of SPIE **6476,** (2007).
3. W. –Y. Chen, R. Grover, T. A. Ibrahim, V. Van, W. N. Herman, and P. –T. Ho, "High-Finesse Laterally Coupled Single-Mode Benzocyclobutene Microring Resonators," IEEE Photon. Tech. Lett. **16,** 470-472, (2004).
4. A. Yeniay, R. Gao, K. Takayama, R. Gao, and A. F. Garito, "Ultra-low-loss polymer waveguides," J. Lightwave Technol. **22,** 154-158, (2004).
5. L. Zuo, H. Suzuki, K. Kong, J. Si, M.M. Aye, A. Watabe and S. Takahashi, "Athermal silica based interferometer type planar lightewave circuits realized by a multicore fabrication method," Opt. Lett. **28,** 1046-1048, (2003).
6. P. Rabiei, W. H. Steier, C. Zhang, and L. R. Dalton, "Polymer Micro-Ring Filters and Modulators," J. Lightwave. Technol., **20,** 1968-1975, (2002).
7. L. A. Eldada, "Polymer integrated optics: promise versus practicality," Proc of. SPIE **4642,** 11-22, (2002).
8. B. Schmidt, Q. Xu, J. Shakya, S. Manipatruni, and M. Lipson, "Compact electro-optic modulator on silicon-on-insulator substrates using cavities with ultra-small modal volumes," Opt. Express **15,** 3140-3148 (2007).
9. H. Fukuda, K. Yamada, T. Tsuchizawa, T. Watanabe, H. Shinojima, and S. -i. Itabashi, "Ultrasmall polarization splitter based on silicon wire waveguides," Opt. Express **14,** 12401-12408 (2006).
10. W. Bogaerts, R. Baets, P. Dumon, V. Wiaux, S. Beckx, D. Taillaert, B. Luyssaert, J. V. Campenhout, P. Bienstman, and D. V. Thourhout, "Nanophotonic Waveguides in Silicon-on-Insulator Fabricated With CMOS Technology," J. Lightwave Technol. **23,** 401-412 (2005).
11. Almeida, V. R., Barrios, C. A., Panepucci, R. R., Lipson, M., "All-optical control of light on a silicon chip," Nature **431**, 1081-1084, (2004).
12. Y. A. Vlasov and S. J. McNab, "Losses in single-mode silicon-on-insulator strip waveguides and bends," Opt. Express **12,** 1622-1631 (2004).
13. S. Kim, J. Jiang, and G. P. Nordin, "Design of compact polymer Mach-Zender interferometer and ring resonator with air trench structures," Opt. Eng. **45,** 54602-54609, (2005).

#90221 - $15.00 USD Received 28 Nov 2007; revised 25 Dec 2007; accepted 2 Jan 2008; published 4 Jan 2008

14. L. Li, G. P. Nordin, J. M. English and J. Jiang, "Small-area bends and beamsplitters for low index-contrast waveguides," Opt. Express **11,** (2003).
15. J. Cardenas, L. Li, S. Kim and G. P. Nordin, "Compact low loss single air interface bends in polymer waveguides," Opt. Express **12,** 5314-5324, (2004).
16. Y. Lin, J. Cardenas, S. Kim and G. P. Nordin, "Reduced loss through improved fabrication for single air interface bends in polymer waveguides," Opt. Express **14,** (2006)
17. J. Ballato and S. H. Foulger and Dennis W. Smith, Jr., "Optical properties of perfluorocyclobutylpolymers. II. Theoretical and experimental attenuation," J. Opt. Soc. Am., B **21,** (2004).
18. J. Ballato, D. W. Smith, Jr, S. Foulger, "Optical properties of perfluorocyclobutyl polymers," J. Opt. Soc. Am. **20 (9),** 1838-1843 (2003).
19. D. W. Smith Jr, S. Chen, S. M. Kumar, J. Ballato, C. Topping, H. V. Shah, and S. H. Foulger, "Perfluorocyclobutyl Copolymers for Microphotonics," Adv. Mater **14 (21),** 1585-1589 (2002)
20. Andrea Guarino, Gorazd Poberaj, Daniele Rezzonico, Riccardo Degl'Innocenti & Peter Günter, "Electro–optically tunable microring resonators in lithium niobate," Nature Photonics **1,** 407 - 410 (2007).
21. W. M. J. Green, R. K. Lee, G. A. DeRose, A. Scherer, and A. Yariv, "Hybrid InGaAsP-InP Mach-Zehnder Racetrack Resonator for Thermooptic Switching and Coupling Contro,".Opt. Express **13,** 1651-1659, (2005).
22. T.P. White, C. M. de Streke, R.C. McPhedran, T. Huang, and L.C. Botton, "Recirculation enhanced switching in photonic crystal Mach-Zehnder interferometers," Opt. Express **12,** 3035-3045, (2004).
23. M. Izutsu, Y. Nakai and T. Sueta, "Operation mechanism of the single-mode optical-waveguide Y junction," Opt. Lett. **17,** 136-138, (1982).
24. D.L. Lee,*Electromagnetic principles of integrated optics*. (New York, John Wiley & Sons, 1986).
25. C.T. Lee and M.L. Wu, "Apexes-Linked circle grating for low-loss waveguide bends," IEEE Photon. Technol. Lett. **13,** 597-599, (2001).
26. N. Rahmanian, S. Kim, G. P. Nordin, "Anisotropic, high aspect ratio etch for perflourocyclobutyl polymers with stress relief technique," J. Vac. Sci. Technol. **24,** 2672-2677, (2006).
27. S. Kim, J. Cai, J. Jiang, and G. Nordin, "New ring resonator configuration using hybrid photonic crystal and conventional waveguide structures," Opt. Express **12**, 2356-2364 (2004).

1. Introduction

Low index contrast (LIC) waveguide materials (core/clad refractive index difference $\leq$1.5%) such as silica and various polymers offer low propagation and fiber coupling losses in addition to well-developed fabrication processes [1-7]. However, waveguide bends and splitters in these materials are relatively large, which severely limits reduction of device size. This has motivated exploration of high index contrast (HIC) material systems such as silicon-on-insulator [8-12]. We have alternatively proposed the use of air-trench splitters [13] and bends [14-16] in LIC materials to make waveguide device size independent of refractive index contrast. In this paper we report the first experimental demonstration of this concept using air-trench splitters. We show as an example very compact ring resonators (RRs) [Fig. 1(a)] in a perfluorocyclobutyl (PFCB) polymer waveguide material system (refractive index contrast 1.3%) [17-19] in which the RR area is reduced by a factor of 1,700 compared to designs with conventional couplers and curved waveguides.

We recently demonstrated that compact bends can be realized in low refractive index, low index contrast (LILIC) materials using air trenches based on adjusting the bend angle to insure that all of the angular spectrum components of the waveguide mode undergo total internal reflection (TIR) [14-16]. For example, using this approach we achieved a measured bend efficiency of 97.2% for TE polarization (electric field in the plane of the substrate) and 96.2% for TM polarization (electric field out of the plane) [16]. We now experimentally show that narrow air trenches can be used to create splitters in which the air-trench partially reflects the incident waveguide mode while the rest of the light is transmitted through frustrated total internal reflection (FTIR). We use PFCB channel waveguides with cross sectional core dimensions of 3.6μm x 3.6μm which insures single mode operation at a wavelength of 1.55μm. All calculations and measurements reported herein are made for the TM polarization mode. Similar results should obtain for TE polarization except the splitting ratio for a given splitter will be slightly different as will the phase shift of the reflected waveguide mode.

#90221 - $15.00 USD Received 28 Nov 2007; revised 25 Dec 2007; accepted 2 Jan 2008; published 4 Jan 2008

Air-trench splitter fabrication is discussed in Section 2. Experimental measurement of splitters and RRs based on air-trench splitters is presented in Section 3. RR measurements are compared with analytical calculations in Section 4 with conclusions presented in Section 5.

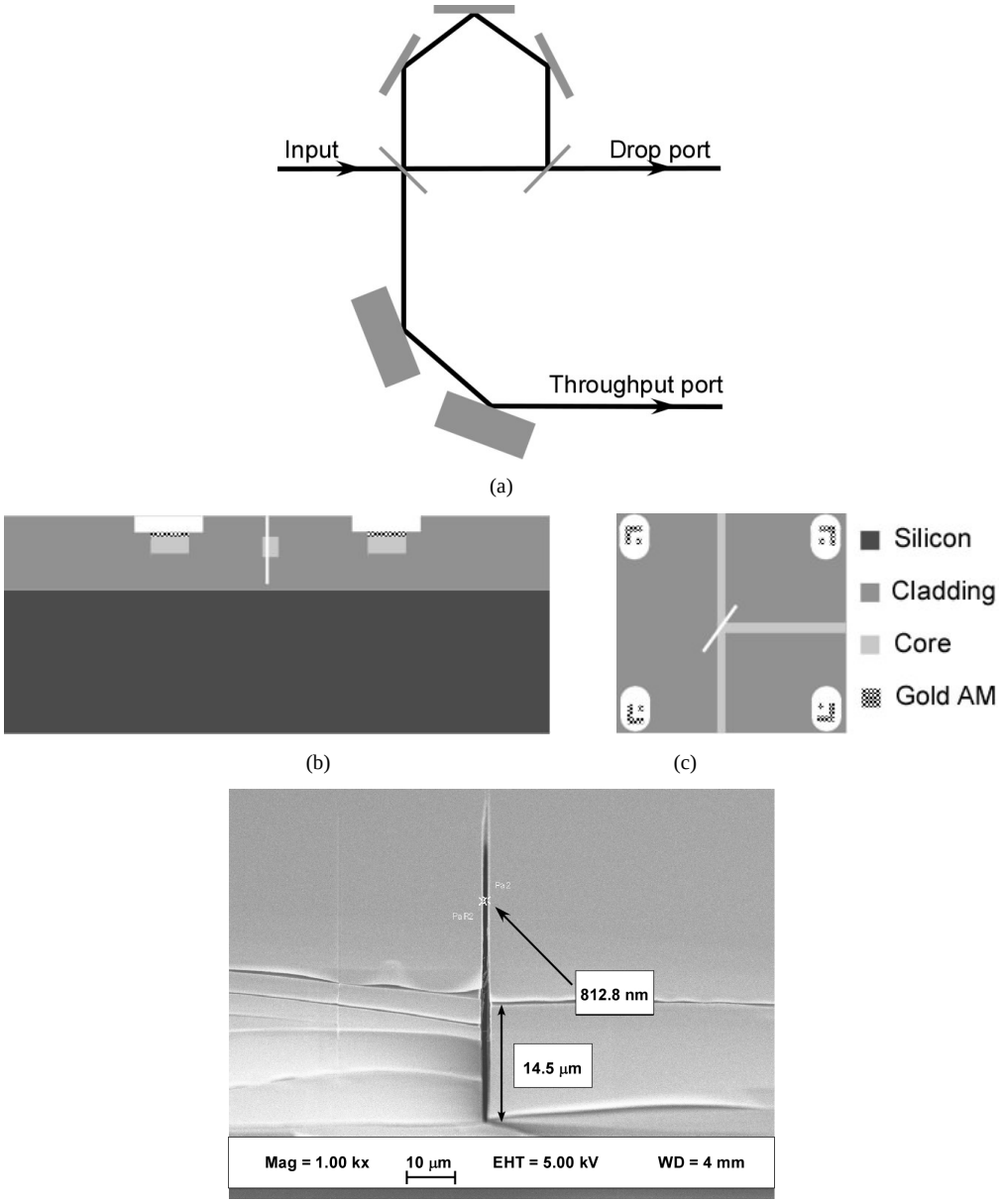

Fig. 1. (a) Schematic illustration of compact ring resonator based on air-trench bends and splitters [after 13] (b) Cross sectional and (c) top view schematic illustrations of fabricated air trench. (d) Scanning electron microscope (SEM) tilted cross sectional view of an etched trench in a PFCB film stack in which there are no waveguides [26]. The trench is etched nearly through the PFCB stack. The thin film on top of the stack that is slightly delaminated along the cleave is the aluminum etch mask, which has not yet been removed.

#90221 - $15.00 USD Received 28 Nov 2007; revised 25 Dec 2007; accepted 2 Jan 2008; published 4 Jan 2008

2. Fabrication

Our PFCB waveguide devices are fabricated on 3" silicon substrates. The undercladding and core layers are spin coated and cured in succession. Waveguides are patterned using contact optical lithography with AZ 701 MiR i-line photoresist to pattern an SiO_2 hard mask that is sputter deposited on the core layer which is then etched in an inductively coupled plasma reactive ion etcher (ICP-RIE) (Surface Technology Systems) using a He/O_2 etch chemistry. The overcladding is next spin coated and cured on top of the waveguides and trenches are patterned in ZEP 520A positive e-beam resist using electron beam lithography (EBL). An aluminum film deposited on the overcladding is used as an etch hard mask. Alignment to the underlying waveguides is accomplished with the aid of gold alignment marks that are patterned in the same step as the waveguides [Figs. 1(b) and 1 (c)]. We use the autoalignment feature of our in-house NPGS version 9 pattern generation system (JC Nabity Lithography Systems) and a LEO 1550 field emission scanning electron microscope (SEM) to obtain an alignment accuracy of less than 40 nm [16].

To experimentally achieve high optical efficiency, fabricated air-trenches must meet very challenging requirements such as vertical and smooth sidewalls for high aspect ratio trenches (18:1) with sub-micron widths. We have developed the necessary etch process and, as reported in Ref. 26, discovered that this is only achievable in PFCB waveguides if the splitter trench is sandwiched between stress relief trenches. Without these extra trenches the splitter trench is widened by tensile stress in the film, which is produced during the thermal curing process because of the coefficient of thermal expansion (CTE) mismatch between the silicon substrate and the PFCB film stack. Figure 1(d) shows a tilted cross sectional scanning electron microscope (SEM) image of an etched trench with the desired trench width, vertical sidewalls, and proper etch depth. The stress relief trenches are outside of the field of view of the SEM image.

Figure 1(a) shows our ring resonator configuration using air-trench bends and splitters. The bends in the ring deflect the incident light by 60° using 1.3 μm wide trenches. Two 45° bends with wider trenches are used in the throughput port path to deflect the waveguide 90° toward the output facet of the chip. Two-dimensional FDTD simulation predicts 99.3% optical efficiency for the 60° bends with an essentially flat spectral response over a wavelength range of 1.5-1.65 μm. Use of these bends in conjunction with air-trench splitters results in a very compact RR size of 100μm x70μm, which is a factor of 1,700 smaller compared to the area required to implement a traditional curved waveguide RR in the same material system (i.e., the minimum bend radius is 2 mm, which results in a ring with an area of 12.6 mm^2 compared to an area of 0.0075 mm^2 for a RR with air trenches).

3. Experimental measurement

We use a Newport PM500 Autoalign System to optically characterize both splitters and RRs. The linearly polarized output of a wavelength tunable laser centered at 1550 nm is used with polarization maintaining (PM) fiber that is butt coupled to each input waveguide in turn. The polarization state of light launched into a waveguide is controlled by rotation of the PM fiber. The proper rotation is set prior to butt coupling by minimizing light through a polarizer oriented orthogonally to the desired linear polarization state. The output optical power from a given waveguide is butt coupled into a single mode fiber, which is connected to an optical power meter. Two computer-controlled precision 3-axis motion stages with 50 nm accuracy are used to optimize the input and output fiber position for highest throughput power. The wavelength is changed in 0.1 nm steps to measure the RR spectral response.

3.1 Air-trench splitters

To characterize air-trench splitter optical performance at 1550 nm we fabricated sets of equal-length waveguides that have different numbers of splitters. Separate sets are used for transmission and reflection measurements. The geometry for reflection is the same as shown in Fig. 4 of Ref. 16 except that the bends are replaced by splitters and the transmission

#90221 - $15.00 USD Received 28 Nov 2007; revised 25 Dec 2007; accepted 2 Jan 2008; published 4 Jan 2008

waveguide for each splitter consists of a short (~10 μm) stub. The geometry for transmission is comprised of a set of straight waveguides, each with a different number of splitters in which the reflection path for each is likewise a short stub. Figures 2(a) and 2(b) show measured reflection and transmission data for splitters with 950 nm wide trenches. The splitter reflection and transmission optical efficiencies are 77.4% and 12.7%, respectively, for a total splitter optical efficiency of 90.1% (i.e., loss of 0.45 dB/splitter).

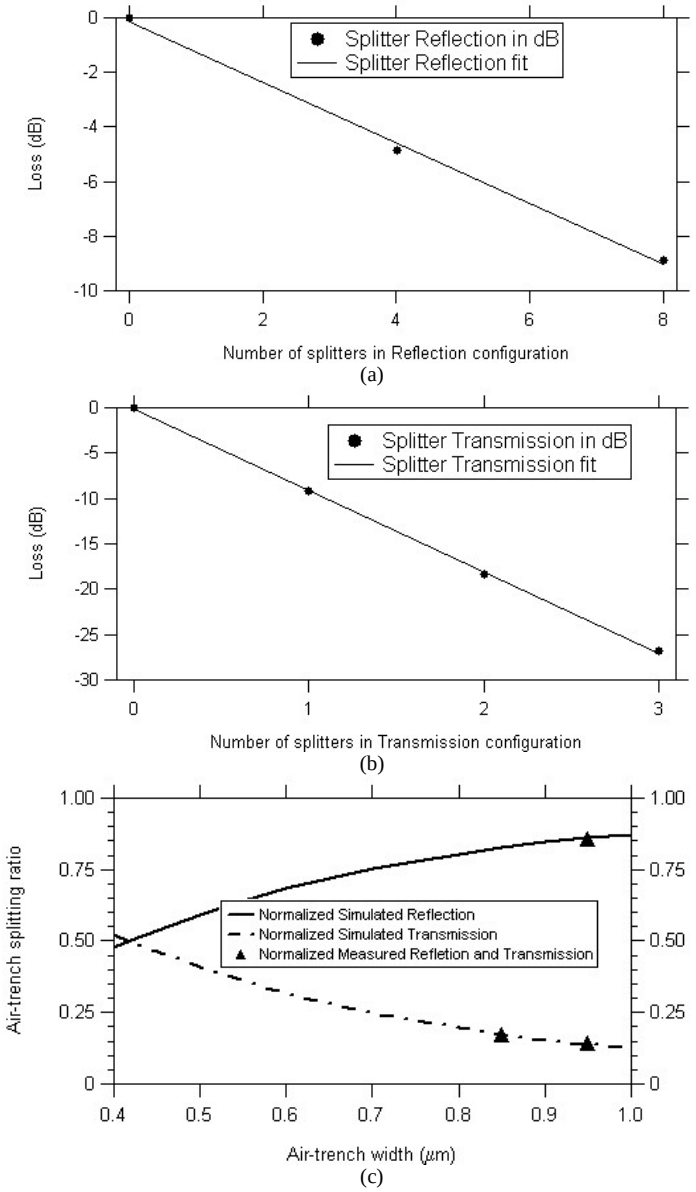

Fig. 2. Splitter efficiency measurement and comparison to simulation results for (a) reflection and (b) transmission for a splitter trench width of 95 nm. The measurements are referenced to the power transmitted through a straight waveguide with no splitters. The error is ±0.02dB for the measured data. (c) Air-trench splitting ratio as a function of air-trench width. Solid and dashed lines represent 2-D FDTD results for reflection and transmission. Measurements are shown as triangular markers.

#90221 - $15.00 USD Received 28 Nov 2007; revised 25 Dec 2007; accepted 2 Jan 2008; published 4 Jan 2008

Figure 2(c) shows the air-trench splitting ratio (i.e., reflected or transmitted optical power divided by the sum of the two) as a function of trench width. The solid and dashed lines are from FDTD simulation while the triangles show measured splitting ratios. The measured reflection/transmission splitting ratios for a trench width of 950 nm are 0.859/0.141, which is in very close agreement with 2-D FDTD simulation results of 0.861/0.139. The measured transmission splitting ratio for a trench width of 850 nm also shows excellent agreement with FDTD predictions (note that there is no measured reflection splitting ratio data point at a 850 nm trench width because of fabrication defects in that particular reflection waveguide set). We believe that the difference in overall measured efficiency (90.1%) compared to the 2-D FDTD simulation result (98.7%) [13] is a consequence of trench sidewall roughness which can be reduced by improvements in the trench patterning and etch processes.

3.2 Ring resonator

A microscope image of a fabricated ring resonator is shown in Fig. 3(a). The splitter trenches are 950 nm wide. Note that the two splitter trenches are sandwiched between stress relief trenches while the bend trenches have stress relief trenches only on the outside of the ring. This is due to lack of space inside the ring to position additional stress relief trenches for the bends.

In order to estimate the optical efficiency of the bends and splitters, additional waveguides with different numbers of bends or splitters are included on the same die. Measurement of splitter reflection and transmission and bend reflection can therefore be made for bends and splitters that have undergone the same fabrication processing conditions as the bends and splitters in the ring resonators. These measurements yield a total splitter efficiency of 84.5% and a bend efficiency of 85.0%. It should be noted, however, that individual bends used in these measurements have stress relief trenches on both sides of each bend whereas each ring resonator bend has only one stress relief trench on the outside of the ring. Measurements of isolated bend trenches (i.e., no stress relief trenches) show a bend efficiency of only ~45%. We expect that the presence of the splitter trenches and their associated stress relief trenches at least partially fulfill the function of stress relief trenches for the RR bends and therefore assume in our calculations in Section 4 that the ring resonator bends have an efficiency approaching 85%. Also note that the total splitter efficiency is somewhat less on this particular die owing to fabrication variations compared to the splitters reported in the previous section.

To characterize the spectral properties of the ring resonator the coupling efficiency is first measured by introducing light into a 1 cm long straight waveguide with a fiber, and then collecting the light exiting the waveguide with a second fiber. The laser power is 1 mW and the measured optical power in the output fiber is 300 μW for a total loss of 5.2 dB. The measured propagation loss for our PFCB waveguides is 0.4 dB/cm (as measured using the waveguide cutback method) so the fiber-waveguide coupling loss is 2.4 dB, which is consistent with measurements of other PFCB waveguide devices in our labs. Using this coupling loss, the absolute drop port and throughput port efficiencies can be measured as a function of wavelength and are shown in Figures 3(b) and 3(c). The measured FSR is 7.1 nm, which is in agreement with 2D FDTD simulation for this RR geometry. Note that the FSR is much larger than can be achieved in a RR comprised of conventional curved waveguides for such a small core/clad refractive index contrast as found in our PFCB waveguides. For example, a circular ring resonator with a 2 mm radius would have a FSR of only 0.13 nm, which is 55 times smaller. The device has a Q of 590, a drop port full width at half maximum (FWHM) of 2.7 nm, and insertion losses of ~11 dB at the drop port (i.e., on resonance) and ~5.5 dB at the through port (i.e., out of resonance). The latter loss is primarily due to defects for this particular sample in the output waveguide between the RR and the output facet of the die.

#90221 - $15.00 USD Received 28 Nov 2007; revised 25 Dec 2007; accepted 2 Jan 2008; published 4 Jan 2008

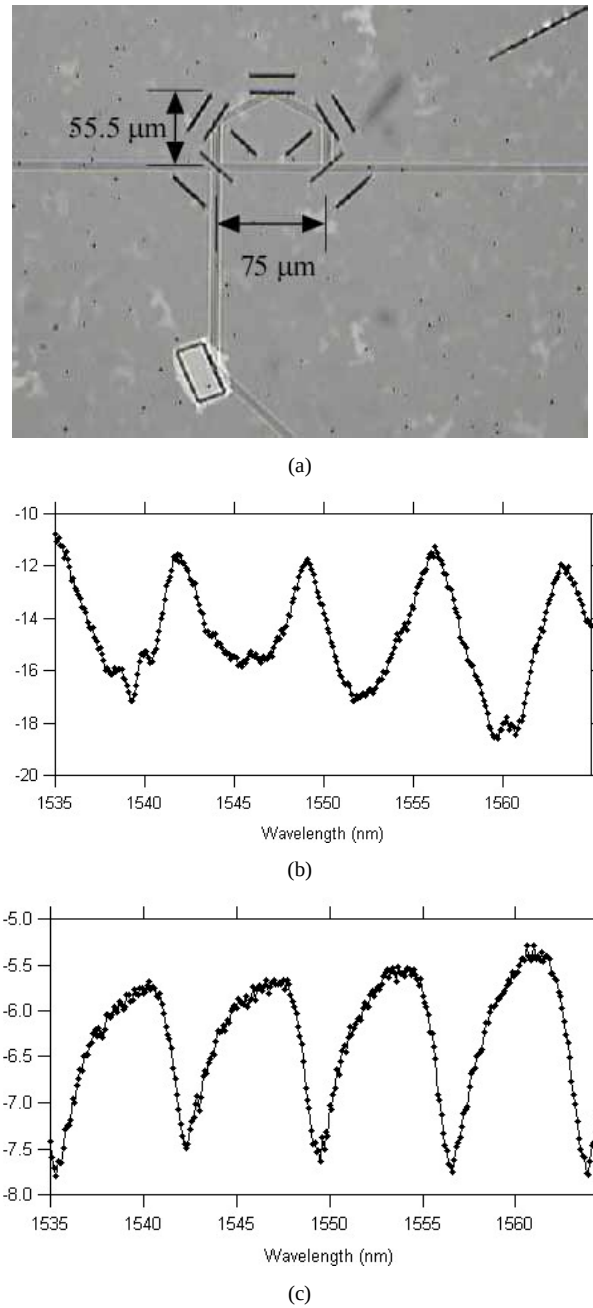

Fig. 3. (a) Microscope image of fabricated RR. Measured (b) drop and (c) throughput port loss.

4. Discussion

The measured RR performance can be compared to results from analytical expressions for the drop and throughput port spectral responses [27], which can be written as

#90221 - $15.00 USD Received 28 Nov 2007; revised 25 Dec 2007; accepted 2 Jan 2008; published 4 Jan 2008

$$T_{drop} = \frac{T_s^2 \Big/ \left(1 - R_s R_b^{1.5}\right)^2}{1 + \left[4R_s R_b^{1.5} \Big/ \left(1 - 4R_s R_b^{1.5}\right)^2 \sin^2\left(\phi/2\right)\right]} \quad (1)$$

$$T_{through} = R_s \left(1 + \frac{T_s^2 R_b^3 - 2T_s R_b^{1.5} \cos(\phi) + 2T_s R_s R_b^3}{\left(1 - R_s R_b^{1.5}\right)^2 + 4R_s R_b^{1.5} \sin^2\left(\phi/2\right)} \right) \quad (2)$$

in which T_s and R_s are the splitter transmission and reflection efficiencies, R_b is the bend efficiency, $\phi = 2\pi n_{eff} d/\lambda + \phi_{sb}$, n_{eff} is the effective refractive index of the waveguide mode, d is the round trip light propagation distance in the ring resonator, and ϕ_{sb} is the phase shift due to reflections from the bends and splitters in one trip around the ring. We assume ϕ_{sb} is zero in the following calculations since we are only interested in comparing losses and extinction ratios.

The calculated drop port and throughput port transmission are shown in Figs. 4(a) and 4(b) for $d = 229.5$ μm, $n_{eff} = 1.47$ (as calculated by determining the effective index of the equivalent two-dimensional waveguide structure for our 3-D waveguide geometry), 84.5% splitter and 85% bend efficiency, and a 85/15 splitting ratio. The FSR is 7.1 nm, in good agreement with measurement. The maximum drop port transmission shown in Fig. 4(a) is -11 dB, which matches the measurement result in Fig. 3(b) and indicates that the bend and splitter efficiencies used in the calculation are in agreement with actual bend and splitter losses. As noted above, defects in the output waveguide of the throughput port and consequent excess loss do not permit comparison of the measured and calculated peak throughput port efficiency. However, the measured throughput port extinction ratio of approximately 2 dB is consistent with the calculated value of ~2.5 dB.

Achieving lower insertion losses and greater extinction ratios requires higher bend and splitter efficiencies. This is illustrated in Figs. 4(c) and 4(d) in which the maximum and minimum drop and throughput port efficiencies are shown as a function of the splitter and bend efficiency, respectively (see caption for details). Note in Fig. 4(c) that the maximum drop port efficiency decreases very rapidly with decreasing splitter efficiency while the maximum throughput port efficiency varies linearly with splitter efficiency. Fig. 4(d) shows that the maximum drop port efficiency is also a very strong function of the bend efficiency. In both cases this illustrates how important overall cavity loss is to obtaining high drop port efficiency. In Fig. 4(d) the maximum throughput port efficiency is only weakly dependent on bend efficiency since the cavity loss does not significantly affect the throughput port transmission when the RR is not in resonance. Figs. 4(c) and 4(d) also illustrate that high extinction ratios for the drop and througput ports require very high splitter and bend efficiencies.

Our previous work [16] has demonstrated 96.2% measured bend efficiency for TM polarized light in PFCB bends while FDTD simulations suggest a maximum possible splitter efficiency of 98.7%. With careful attention to fabrication process optimization it should therefore be possible to obtain bend and splitter efficiencies of 95% or more. In this case very attractive ring resonator properties can be obtained in low index contrast waveguides. For example, calculation shows that a RR with 95% bend and splitter efficiency and the same size as the RR reported in this paper will have a FWHM of 0.65 nm and a Q of 2,400 with a drop port loss of 5 dB and a drop port extinction ratio of 17 dB.

#90221 - $15.00 USD Received 28 Nov 2007; revised 25 Dec 2007; accepted 2 Jan 2008; published 4 Jan 2008

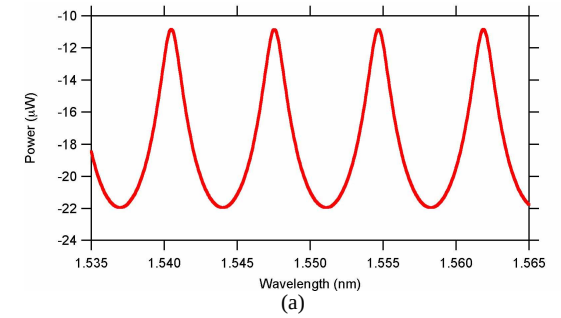

(a)

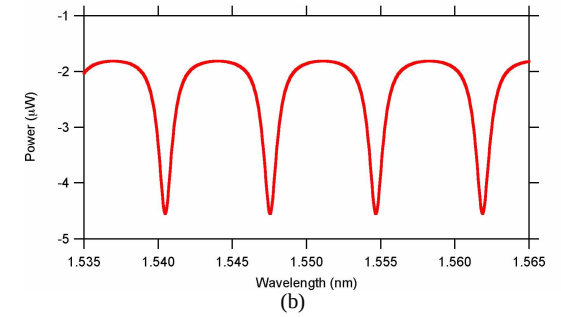

(b)

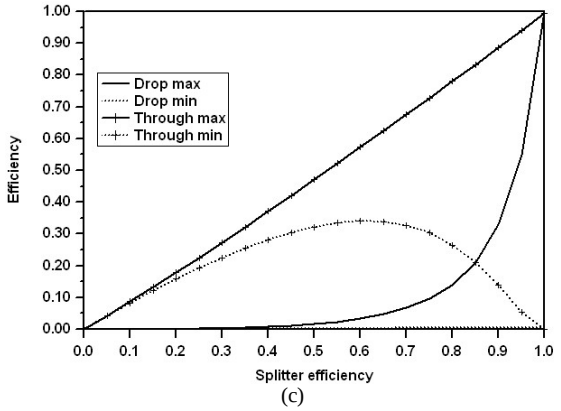

(c)

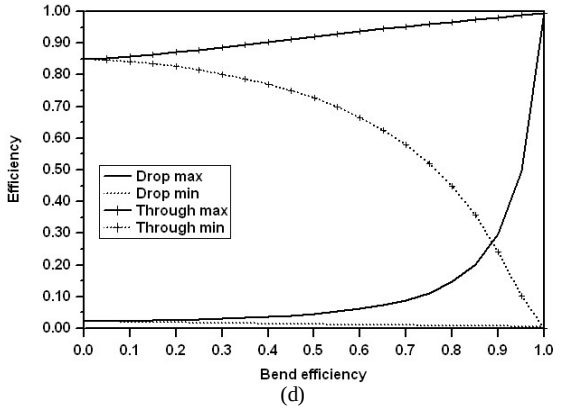

(d)

Fig. 4. Analytically calculated RR (a) drop and (b) throughput port losses as a function of wavelength for a RR with 84.5% splitter and 85% bend efficiency and a 85/15 splitting ratio. Maximum and minimum drop and throughput port efficiencies as a function of (c) splitter efficiency assuming unity bend efficiency and (d) bend efficiency assuming unity splitter efficiency.

#90221 - $15.00 USD Received 28 Nov 2007; revised 25 Dec 2007; accepted 2 Jan 2008; published 4 Jan 2008

5. Conclusion

Compact 90^o splitters are demonstrated in low index contrast PFCB waveguides through use of air trenches. Comparison between 2D FDTD simulation results and measured splitting ratios shows close agreement. The measured 0.4dB splitter loss is likely due primarily to air-trench sidewall roughness, which can be alleviated by further improvements in the fabrication process. An ultra-compact ring resonator is demonstrated based on air-trench splitters and bends, which reduces RR size by 1,700 compared to a comparable RR realized with traditional curved waveguides.

Acknowledgment

This work was supported in part by DARPA grant N66001-04-8933.

#90221 - $15.00 USD Received 28 Nov 2007; revised 25 Dec 2007; accepted 2 Jan 2008; published 4 Jan 2008